NJC

ROYAL SOCIETY OF CHEMISTRY

PAPER

Cite this: *New J. Chem.*, 2022, **46**, 16547

Stereoselective quantitative analysis of ranolazine in plasma and tissue samples: application in pharmacokinetics and tissue distribution studies†

Yuanyuan Zhu,[a] Hong Zhang, *[b] Siman Ma,[a] Lizhi Miao,[c] Ge Jin,[d] Jiahui Li,[e] Tohutanguli Nuerkaman,[e] Qiruo Sun,[a] Yang Liu[d] and Shiliang Yin*[d]

This study aimed to develop a rapid and sensitive reversed-phase mode high-performance liquid chromatography-electrospray ionization coupled with a tandem mass spectrometry method for the simultaneous determination of ranolazine enantiomers in rat plasma and tissues. The obtained biological samples were pretreated with the liquid–liquid extraction method, and methyl *tert*-butyl ether was employed as the extracting agent. The efficient stereo separation of target compounds was achieved on a Chiralcel OD-RH column by using the mobile phase consisting of acetonitrile–2 mM aqueous ammonium acetate (80 : 20, v/v) at a flow rate of 0.6 mL min^{-1}. The analytes were detected by multiple reaction monitoring in positive ion mode with the mass transitions at *m/z* 428.20 > 279.50 (ranolazine) and 219.80 > 128.06 (ornidazole, internal standard). Furthermore, the elution peak order on the Chiralcel OD-RH column was confirmed by the recorded and calculated electronic circular dichroism spectrum. The results of this pharmacokinetic study revealed that the C_{max} and AUC_{0-t} values of *R*-(+)-ranolazine were 2.05 and 2.72 times higher than those of *S*-(−)-ranolazine. Compared with *S*-(−)-ranolazine, *R*-(+)-ranolazine displayed stronger absorption capability in rat plasma and a slower metabolism rate in major organs of rats. The highest content of *R*-(+)-ranolazine was in the liver, followed by the kidneys, heart, lungs and spleen. It is noteworthy that this is the first stereoselective report regarding the pharmacokinetics and tissue distribution of ranolazine *in vivo*, which may benefit instructing the clinical application for safer treatment.

Received 10th May 2022,
Accepted 26th July 2022

DOI: 10.1039/d2nj02302d

rsc.li/njc

1. Introduction

Ranolazine, a piperazine derivative, is a proven *anti*-ischemia and *anti*-anginal agent for the treatment of chronic stable angina with negligible effects on the heart rate and blood pressure.[1–3] It acts primarily by inhibiting the later sodium current to decrease the calcium overload and thus reducing ischemia and angina symptoms.[4–8] In clinical practice, ranolazine is orally administered as a racemic compound.[9] The chemical structures of ranolazine enantiomers are demonstrated in Fig. 1.

Chemically, ranolazine contains a stereogenic center, leading to a pair of enantiomers. It is prominent that for most chiral compounds, only one enantiomer is pharmacologically active but the other may be inactive or exert completely diverse activity secondary to the stereoselective binding effects of each enantiomer with biological macromolecules (such as enzymes, proteins, and nucleic acids).[10–12] For ranolazine, the *S*-enantiomer displayed stronger *anti*-anginal and *anti*-ischemic activities than the *R*-enantiomer or *rac*-ranolazine whereas the *R*-form improved the glucose levels in diabetic rats by preserving the β-cells and enhancing the secretion of insulin.[13,14] Aside from different biological activities to target objects, the absorption and distribution processes of chiral drugs in organisms are typically

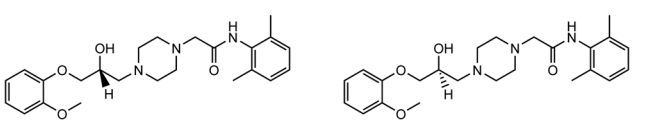

R-(+)-ranolazine *S*-(-)-ranolazine

Fig. 1 Chemical structures of ranolazine enantiomers.

[a] *School of Pharmacy, Shenyang Pharmaceutical University, Shenyang, Liaoning, 110016, China*
[b] *School of Life Science and Biopharmaceutics, Shenyang Pharmaceutical University, No. 103 Wenhua Road, Shenyang 110016, China. E-mail: song0688@sina.com*
[c] *Safety Evaluation Center of Shenyang SYRICI Testing Co., Ltd., Shenyang 110141, China*
[d] *School of Pharmacy, Shenyang Medical College, No. 146 Huanghe North Street, Shenyang, Liaoning, 110034, China. E-mail: yslal@163.com*
[e] *School of Business Administration, Shenyang Pharmaceutical University, Shenyang 110016, China*

† Electronic supplementary information (ESI) available. See DOI: https://doi.org/10.1039/d2nj02302d

stereoselective.[15,16] Although, research on the stereoselective behavior of ranolazine *in vivo* is scarce, several analytical methods have already been established for the detection of ranolazine in biological samples. These methods mainly include high-performance liquid chromatography (HPLC),[17] high performance thin-layer chromatography-mass spectrometry (HPTLC-MS),[18] liquid chromatography-tandem mass spectrometry (LC-MS/MS),[19–21] and spectrophotometric methods.[22] However, it is noteworthy that these methods mainly focus on the study of racemates. Therefore, it is necessary to establish a sensitive and rapid analytical method to determine the concentration of ranolazine enantiomers in biological samples to investigate their enantioselectivity *in vivo*.

So far, few HPLC methods have been reported for chiral separation of ranolazine enantiomers.[9,23–25] Accompanied by high-resolution efficiency and universal applicability, the HPLC method based on chiral stationary phases (CSPs) was widely used as an effective method of chiral separation.[11,26,27] Luo *et al.* developed a chiral HPLC method using a cellulose tris (3,5-dimethylphenylcarbamate) CSP under both normal-phase and polar organic phase modes for the analysis and resolution of ranolazine enantiomers; however, it lacked sufficient sensitivity for bioanalytical applications (lower limit of quantitative (LLOQ) of 2.9 mg mL^{-1}).[9] Additionally, Gao *et al.* reported a multifunctional immobilized CSP based on dialdehyde microcrystalline cellulose for separating ranolazine enantiomers in reversed-phase mode. The separation factor (α) and resolution values (R_s) were slightly low (α = 1.55 and R_s = 0.82).[23] Another study used a Chiralcel OD-H column in normal-phase mode to determine the enantioselectivity of ranolazine in rat liver microsomal fractions, and the complete separation was accomplished within 17 min.[25] However, as one of the components of the mobile phase, hexane was not suitable for the enantiomeric analysis of ranolazine enantiomers owing to their poor solubility in hexane,[9] and the normal-phase solvents were incompatible for high-performance liquid chromatography with tandem mass spectrometry (HPLC-MS/MS) analysis.[28] Therefore, an HPLC-electrospray ionization coupled with an MS/MS (HPLC-ESI-MS/MS) method under the reversed-phase condition is likely to be ideal for the pharmacokinetics and tissue distribution studies of *rac*-ranolazine *in vivo* to comprehensively investigate the enantioselective behavior of low concentration ranolazine stereoisomers in plasma and tissue samples.

This study aimed to establish an HPLC-ESI-MS/MS method and validate and apply it to determine the pharmacokinetic properties of ranolazine enantiomers in rat plasma and tissues by using liquid–liquid extraction (LLE) technology. First, baseline separation of *R*-(+)-ranolazine and *S*-(−)-ranolazine was achieved on a Chiralcel OD-RH column. Second, we used circular dichroism (CD) spectra to determine the absolute configuration according to the absorption difference between left and right circularly polarized light.[29] In this study, the factors affecting the enantioseparation of ranolazine, including types of chiral columns, the types and contents of the mobile phase, and the proportions of buffer solution, and the sample preparation methods were explored. Compared with Simões's method,[25] our method achieved a much shorter retention time under the reverse-phase mode (t < 6 min). Finally, the optimized analytical method was utilized to carry out the enantioselective pharmacokinetics and tissue distribution following oral administration of 15 mg kg^{-1} *rac*-ranolazine extended-release tablets. The objective of this study was to explore the stereoselectivity of ranolazine enantiomers *in vivo* and their therapeutic efficacy and safety.

2. Materials and methods

2.1 Chemicals and reagents

rac-Ranolazine extended-release tablets were provided by Jingfeng Pharmaceutical Co., Ltd (Hunan, China). Standards of *rac*-ranolazine and *rac*-ornidazole (internal standard, IS) were obtained from the National Institute for the Control of Pharmaceutical and Biological Products (Beijing, China). All standards were ≥98.0% purity. Sigma-Aldrich (Shanghai, China) supplied MS-grade solvents including ammonium hydrogen carbonate, ammonium acetate, methanol (MeOH), and acetonitrile (ACN). MS-grade water was purified using a Milli-Q Water Purification System (Millipore, MA, USA). Other analytical grade reagents were purchased from Yuwang Industrial Co., Ltd (Shandong, China). The solid-phase extraction columns were purchased from Waters Corporation (Waters, Co., Milford, MA, USA).

2.2 Preparation of stock and working solutions

Stock solutions containing 1 mg mL^{-1} *rac*-ranolazine or IS were prepared in ACN, respectively. Ranolazine stock solution was further diluted with ACN to obtain the working standard solutions ranging from 20 to 5000 ng mL^{-1} for individual enantiomers. Similarly, 2000 ng mL^{-1} of IS solution was yielded by diluting the IS stock solution with ACN. All these solutions were kept at 4 °C prior to use.

Meanwhile, 100 μL of blank rat plasma and tissue homogenate were separately mixed with 10 μL of the corresponding *rac*-ranolazine working standard solution and 10 μL of IS working solution for constructing the calibration curves. Following the above-mentioned, the ranges of final plasma concentrations (2–100 ng mL^{-1}) and tissue concentrations (2–200 ng mL^{-1} for heart, spleen and lungs; 2–250 ng mL^{-1} for kidneys; 2–500 ng mL^{-1} for liver) for each ranolazine enantiomer were obtained. Similarly, the quality control samples at low (LQC), medium (MQC) and high (HQC) concentration levels for individual enantiomers were prepared for method validation analysis of plasma and tissue samples. The concentrations of QC samples are as follows: 6, 40 and 80 ng mL^{-1} for plasma samples; 6, 80 and 160 ng mL^{-1} for heart, spleen and lungs; 6, 200 and 400 ng mL^{-1} for the liver; 6, 100 and 200 ng mL^{-1} for the kidneys. All solutions were stored at 4 °C.

2.3 Apparatus and chromatographic conditions

An Agilent 1200 series HPLC system (Agilent Technologies, Santa, Clara, CA, USA) consisting of a binary system,

autosampler and thermostatic column compartment was used for separating ranolazine enantiomers. The optimized enantiomeric resolution was achieved with a mobile phase of ACN-2 mM aqueous ammonium acetate (80 : 20, v/v) at a flow rate of 0.6 mL min^{-1} on the Chiralcel OD-RH column (150 mm × 4.6 mm, 5 μm, Daicel, Japan) coupled with a Chiralcel OD-RH guard column (10 mm × 4.0 mm, 5 μm) under the reversed-phase mode. The column oven and auto-sampler temperature were set at 25 °C and 4 °C, respectively, and the injection volume was 10 μL.

The mass spectrometric detection was performed on an API 4000 triple quadrupole instrument (AB Sciex, Foster City, CA, USA) in multiple reaction monitoring modes. ESI in positive ion mode was applied for detecting ranolazine enantiomers. The MS parameters were optimized to achieve maximum sensitivity. The ion-pair transitions of m/z 428.20 > 279.50 for ranolazine enantiomers were monitored (cone voltage (CV) defined at 5 V and collision energy (CE) at 23 eV). For IS, the monitored mass transition was m/z 219.80 > 128.06 (CV = 20 V, CE = 30 eV).

2.4 Pretreatment of biological samples

For the LLE method, methyl *tert*-butyl ether (MTBE) was selected to extract the ranolazine enantiomers from biological samples. To prepare samples for analysis, 10 μL of IS working solution (2000 ng mL^{-1}) and 100 μL aliquot of plasma or tissue homogenate samples were mixed in MTBE and vortexed for 3 min. Following 12 000 rpm centrifugation for 10 min, the obtained supernatant was transferred to another polypropylene microcentrifuge tube and evaporated to dryness under a gentle stream of nitrogen at 37 °C. Thereafter, the residue was reconstituted in 100 μL of mobile phase (vortex for 1 min) and filtered through a 0.22 μm nylon syringe filter prior to HPLC-ESI-MS/MS analysis.

2.5 Method validation

The method validation was carried out for specificity, carry-over, linearity, LLOQ, precision, accuracy, extraction recovery, matrix effect and stability in accordance with the USA Food and Drug Administration guidelines for the validation of bioanalytical methods.[30]

2.5.1 Specificity and carry-over. The assay of specificity was assessed by comparing chromatograms of six different batches of blank plasma and tissues with those of corresponding standard plasma and tissue samples spiked with ranolazine at the LLOQ level and actual samples (0.5 h for plasma; 12 h for kidneys) from Sprague-Dawley (SD) rats following oral administration of 15 mg kg^{-1} *rac*-ranolazine extended-release tablets. The acceptance criterion for this method was that the peak area of the interference in the retention window of the tested compounds and IS should be <20% of that for the analyte at the LLOQ level and lower than 5% of IS.

The carry-over effect was evaluated by injecting two blank samples directly after detecting the highest concentration standard in each calibration curve analysis run. In the chromatogram of the blank biological samples, the response of any interference should not exceed 20% of the LLOQ response and 5% of the response for the IS at the corresponding retention time.

2.5.2 Linearity and LLOQ. To evaluate the linearity, the calibration curves consisting of seven non-zero concentration levels were established and fitted with a weighted ($1/x^2$) least-squares linear regression line ($y = ax + b$; y: peak area ratios of the individual ranolazine enantiomer to IS; x: the theoretical concentrations in plasma or tissue samples). A correlation coefficient (r^2) of 0.990 or higher was expected for all calibration curves, and the back-calculated standard concentrations should be within 15% deviation from the nominal value except at the LLOQ level. The lowest concentration on the calibration curve is defined as the LLOQ level (signal-to-noise ratio not <10 for quantification). Six individual samples spiked with ranolazine at the LLOQ level were assessed for the analysis of accuracy and precision. Accuracy should be within ±20%, and precision should be >20% to be acceptable.

2.5.3 Precision and accuracy. The inter-day precision and accuracy of this bioanalytical method were validated by determining six replicates of QC samples at four concentration levels (LLOQ, LQC, MQC, and HQC) on three consecutive days. The intra-day precision and accuracy were determined within a day. The precision of this method was defined by calculating the relative standard deviation (RSD) and expected to be <15% except for LLOQ where it should not be >20%. Similarly, accuracy, described as a relative error (RE), should be within ±20% for LLOQ and ±15% for the remaining QC samples.

2.5.4 Extraction recovery and the matrix effect (ME). The extraction recovery of ranolazine enantiomers was investigated by comparing the mean peak area of the extracted spiked samples with the peak area of post-extraction spiked samples. This procedure was performed by analyzing six replicates at three QC levels. The matrix effects of analytes and IS were measured by comparing the peak areas of post-extracted spiked samples with those in the neat standard solutions at three QC levels in six replicates. The normalized matrix factor (NMF) was calculated using the following formula, and the acceptance RSD of NMF was ≤15%.

$$\text{NMF (\%)} = \text{ME}_{\text{analyte}}/\text{ME}_{\text{IS}} \times 100\%$$

2.5.5 Stability. The stability of the analytes was assessed by analyzing six replicates at three QC levels kept on storage for 12 h at room temperature, for 30 days at −80 °C, and 24 h in the autosampler tray at 4 °C. The freeze–thaw stability of ranolazine enantiomers and IS in the plasma and tissue homogenate was evaluated by conducting three freeze–thaw cycles from −80 °C to room temperature for 30 days. Samples were considered stable if the values of RE were within ±15% and RSD was <15%.

2.6 Stereoselective pharmacokinetic study and tissue distribution

Our method was used to study the enantioselective pharmacokinetic profiles of ranolazine following oral administration of 15 mg kg^{-1} *rac*-ranolazine extended-release tablets. All animal

tests in this report were approved by the Ethics Committee of the Animal Experiments of Shenyang Pharmaceutical University (permit number, SYPU-IACUC-C2021-6-13-227).

2.6.1 Animals. Adult male SD rats (260–300 g) were purchased from the Experimental Animal Center of Shenyang Pharmaceutical University (License No. SCXK-Liao-2020-0001, Shenyang, China). The rats were naturally fed for a week in a temperature and humidity-controlled room with a 12 h light–dark cycle and fasted for 12 h prior to drug administration with water arbitrarily made available throughout the experiment.

2.6.2 Experimental design. Both the control group and experimental groups consisted of six randomly assigned male SD rats. 15 mg kg^{-1} *rac*-ranolazine extended-release tablets were orally administered to the rats in experimental groups. Furthermore, blood samples were collected from the retro-orbital plexus of rats at 0 (prior to dosing), 0.25, 0.5, 1, 2, 4, 6, 8, 12, 24 and 48 h following administration. The blood samples were immediately centrifuged at 5000 rpm for 10 min to obtain plasma. Finally, each supernatant plasma layer was harvested.

Twenty-four rats were classified into four groups with six male SD rats in each. The tissues (the heart, liver, spleen, lungs, and kidneys) were excised from these rats at 5, 12, 24 and 48 h following oral administration, and placed in 0.9% sodium chloride solution to remove the blood and weighed separately after wiping with filter paper. The obtained plasma collection and tissues were frozen at −20 °C until further usage.

2.6.3 Data analysis. The enantioselective pharmacokinetic parameters of ranolazine enantiomers were analyzed by a non-compartmental method using the Data Acquisition Software (DAS) (Version 2.0, China). The paired *t*-test, with 95% confidence intervals, was performed to evaluate the difference of parameters between two enantiomers using the SPSS Statistics Software (Version 19.0, Chicago, USA). For p-value < 0.05, differences were significant.

3. Results and discussion

3.1 Sample preparation

Developing a satisfactory and stable sample pretreatment technique, which could not only leads to the optimal recovery and good reproducibility but also effectively reduces the effect of the coexisting interferent, helps prolong the life of a chiral chromatographic column. In our study, three commonly reported sample preparation methods of protein precipitation (PPT), solid-phase extraction (SPE), and LLE for biological analysis were thoroughly assessed.

Our findings for the PPT method demonstrated that the matrix suppression effect was significant whether MeOH or ACN was used as the precipitation solvent. Despite the relatively high recoveries provided by the PPT method, the method validation failed owing to a worse matrix effect. Therefore, we paid more attention to the optimization of SPE and LLE to further account for the possibility that the introduction of a large number of endogenous components into the chiral column would cause damage to the column, we therefore paid more attention to the optimization of SPE and LLE, and the final recoveries are provided in Fig. S1 (ESI†). During the SPE procedure, four available SPE cartridges including Cleanert C_{18}, NH_2, PCX and HLB (Waters, 500 mg, 3 mL) were compared. The processes of the SPE technique are described as follows: 100 μL of blank plasma spiked with 10 μL of standard working solution and 10 μL of IS was vortexed for 1 min and further loaded into four separate cartridges attached to a vacuum manifold (VacElute, Harbor City, CA, USA) and preconditioned with 2 mL of MeOH. After cleaning with 2 mL of deionized water containing 5% MeOH, the vacuum was also applied to the cartridge for 2 min to dry the resin completely. Finally, the studied chemicals were eluted with 2 mL of ACN into a tube. The eluent was dried at room temperature, and the residue was reconstituted with a 100 μL mobile phase. After filtering through a 0.22 μm nylon syringe filter, an aliquot of 10 μL was injected into the analytical system for HPLC-ESI-MS/MS analysis. The results revealed that even though the samples were cleaner, the recoveries from this procedure were worse. In comparison with NH_2, C_{18} and PCX, the relatively higher recovery values extracted by the HLB cartridge were not $>85\%$ (Fig. S1-A, ESI†). Lower recoveries, high cost, and time requirements eventually led to the abandonment of the SPE technique.

In the development of LLE, the selection of suitable extraction solvents has been an analytical challenge. The most widely applied solvents in various forms, such as *n*-hexane-isopropanol (*n*-hexane-IPA) (95 : 5, v/v), ethyl acetate (EtAC), diethyl ether-dichloromethane (DEE-DCM) (60 : 40, v/v) and MTBE, were comprehensively evaluated to obtain the optimal extraction recovery and a relatively low matrix effect in our study. The detailed LLE procedures are described in Section 2.4 ''Pretreatment of biological samples''. As displayed in Fig. S1-A, (ESI†) we observed that the most satisfactory recovery value ($>95\%$) was obtained by employing MTBE as the extraction solvent. To further shorten the sample preparation time, the volume of extraction solvent ranging from 1 to 5 mL was subsequently evaluated. The results (Fig. S1-B, ESI†) suggested that the extraction efficiency steadily increased with the volume of extraction reagent from 1 mL to 3 mL. The recoveries remained stable as the polar solvent volume was increased to 5 mL. Conclusively, the LLE methodology was determined to be an effective method for the extraction of ranolazine enantiomers from plasma and tissues since it required less time, was a less toxic solvent, produced less background noise, and had a higher extraction recovery rate.

3.2 Optimization of the HPLC conditions

To efficiently separate ranolazine enantiomers, we initially tested three commercialized immobilized polysaccharide-based CSPs under the reversed-phase mode, including Chiralpak IH, Chiralpak IC and Chiralcel OD-RH columns. However, the Chiralpak IH column could not achieve the baseline separation of ranolazine enantiomers during the whole screening. As presented in Fig. 2, after trialing different mobile phase compositions and additives, Chiralpak IC performed chiral

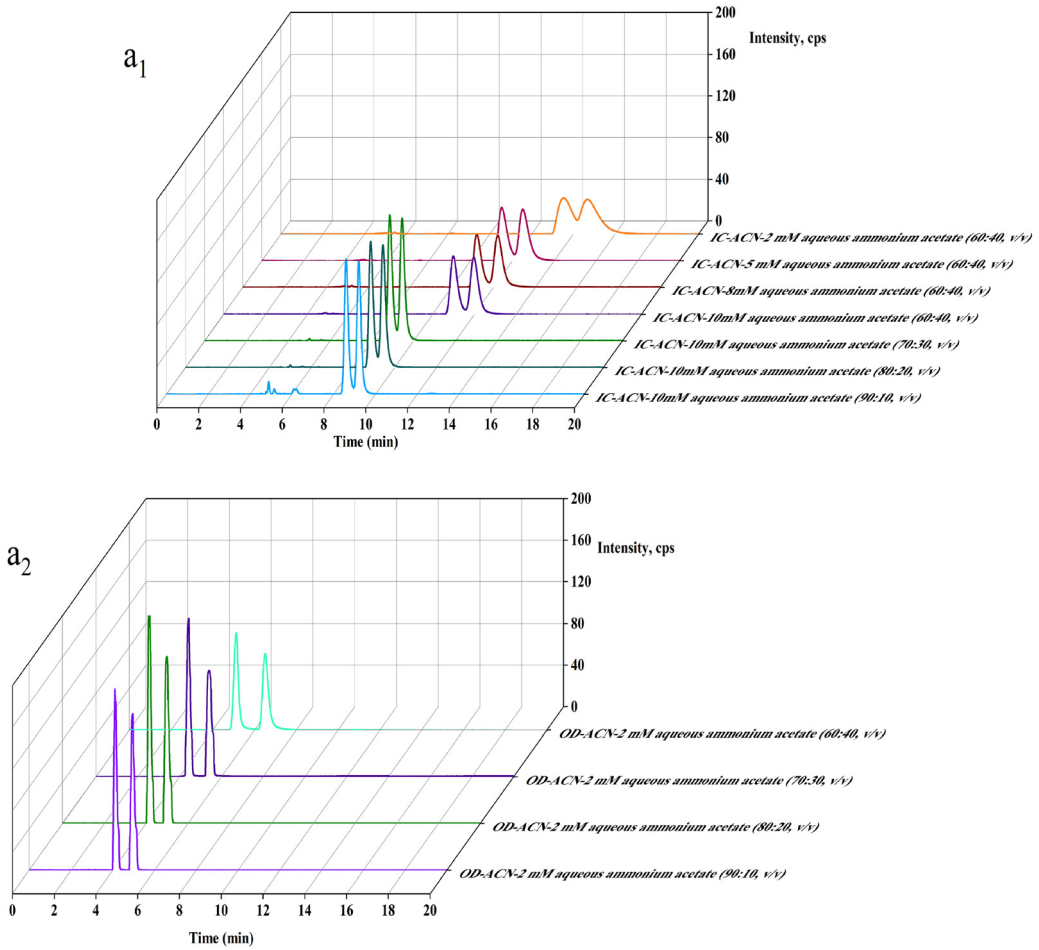

Fig. 2 Effect of chiral columns, contents of the mobile phase, and the proportions of buffer solution on the chromatographic response of ranolazine enantiomers.

recognition capability towards *rac*-ranolazine. Under the same conditions, the Chiralcel OD-RH column outperformed Chiralpak IC in terms of the target analyte resolution, peak shape, shorter running time, and signal response. Thus, the Chiralcel OD-RH column was selected to further optimize the enantiomeric separation of ranolazine.

Considering the effects of the mobile phase on resolution, CSP stability and column lifespan, we tested the components and proportions of the mobile phase under the reversed-phase mode. In this study, MeOH and ACN were tested as organic modifiers of the mobile phase. The results suggested that MeOH or ACN did not resolve ranolazine enantiomers without any additives and the column pressure significantly increased when MeOH was used. Hence, a volatile buffer salt such as ammonium acetate was used to improve the resolution of ranolazine. When MeOH-aqueous ammonium acetate was used as the mobile phase, there was no improvement in resolution in either Chiralcel OD-RH or Chiralpak IC column. However, the employment of ACN exhibited a high response and symmetric peak shape owing to the addition of ammonium acetate. Moreover, our results revealed that the ionic strength (2, 5, 8, and 10 mM) of ammonium acetate in ACN did not significantly affect the retention and resolution of target compounds in the Chiralpak IC column (Fig. 2-a_1). For the Chiralcel OD-RH column, when the selected mobile phase contained ACN-2 mM aqueous ammonium acetate (60 : 40, v/v), an acceptable resolution (R_s = 2.562) for both isomers of ranolazine was achieved within 10 min. Afterward, the ACN percentage in the mobile phase was investigated over the range of 60–90% and the chromatograms of the chiral separation of ranolazine on the Chiralcel OD-RH column are presented in Fig. 2-a_2. After complete optimization, a mobile phase consisting of ACN-2 mM aqueous ammonium acetate (80 : 20, v/v) was selected in this method owing to the accredited chromatographic resolution of ranolazine enantiomers (R_s = 2.215). Our method, which achieved a much shorter retention time under the reverse-phase mode (t < 6 min) than Simões's method,[25] can significantly reduce the analysis time for the quantitation of ranolazine in bulk biological samples.

Although the polysaccharide-based CSPs have achieved excellent enantioselectivity for various racemates, the chiral recognition mechanism at the molecular level remains obscure. The differences in ranolazine stereoisomers between Chiralpak IC and Chiralcel OD-RH columns may be owing to the

substituent on the phenyl groups of polysaccharide-based CSPs. For Chiralcel OD-RH, methyl is the substituent on phenyl groups. It is also an electron-donating group that can increase the electron density at the carbonyl oxygen atom of the carbamates. Therefore, alcohol groups near the chiral center of the ranolazine molecule can be greatly absorbed by the CSPs through a hydrogen-bonding interaction. Besides, the presence of aromatic functions of racemates may provide an additional stabilizing effect on the ranolazine–CSP complex by insertion of the aromatic portion into the chiral cavity for the satisfactory stereospecific separation of ranolazine.[31] Additionally, dipole–dipole interactions between the carbonyl groups on the enantiomers and polysaccharide CSPs may contribute to chiral resolution. Chiral polymers usually contain various binding sites with varying affinities to enantiomers making it harder to assess a precise mechanism for the recognition of chirality on the polymeric CSPs.[32] Thus, the Chiralcel OD-RH column was adopted for subsequent optimization steps.

3.3 Optimization of mass spectrometry conditions for quantitative analysis

Mass spectrometry conditions were carefully optimized for determining ranolazine enantiomers in rat plasma and tissue samples. In the scan mode experiment, a greater and stabler MS signal response for each analyte was observed under the positive ionization mode than those under the negative mode. The most abundant ions were protonated molecule ions $[M + H]^+$ at *m*/*z* 428.20 and 219.80 for ranolazine and IS, respectively. Furthermore, two major fragment ions for ranolazine and IS were identified at *m*/*z* 279.50 and 128.06. Therefore, quantification of ranolazine and IS were evaluated in the positive mode and the monitored mass transitions were *m*/*z* 428.20 > 279.50 for ranolazine and *m*/*z* 219.80 > 128.06 for IS. The other instrument parameters were optimized to maximize the sensitivity of the method. The mass spectra are presented in Fig. S2 (ESI†).

3.4 Validation of the elution order and absolute configuration

Chromatographic retention in the separation of chiral chemicals was associated with the free energy of the partitioning process of the analyte between the mobile phase and CSPs. Changes between the mobile phase and CSPs and inversions in the elution of the enantiomers may also occur.[33,34] Although some studies have reported the elution order of ranolazine under the normal-phase mode,[9] there is no information on the confirmation of ranolazine enantiomers eluted on the Chiralcel OD-RH column under the reverse-phase mode. Therefore, determining the elution order and absolute configuration of ranolazine is crucial.

The pure enantiomer of ranolazine was obtained under the optimized HPLC conditions, as presented in Section 3.2, and concentrated in anhydrous MeOH to a suitable concentration of 0.3 mg mL^{-1}. Furthermore, the measurement of the optical rotation for ranolazine enantiomers was carried out on a MOS-450 CD spectrometer using a quartz cuvette with a 1 cm optical path (Jasco, Tokyo, Japan). As displayed in Fig. 3, the first eluted isomer (black line) demonstrated a negative ban at a wavelength of 230 nm, whilst the second eluted peak (red line) demonstrated a positive ban. To further validate the absolute configuration of ranolazine enantiomers, the electronic circular dichroism (ECD) spectra were calculated by the time-dependent density functional theory. Comparing the calculated and experimental results, *R*-(+)-ranolazine corresponded to the first eluted peak and *S*-(−)-ranolazine corresponded to the second peak.

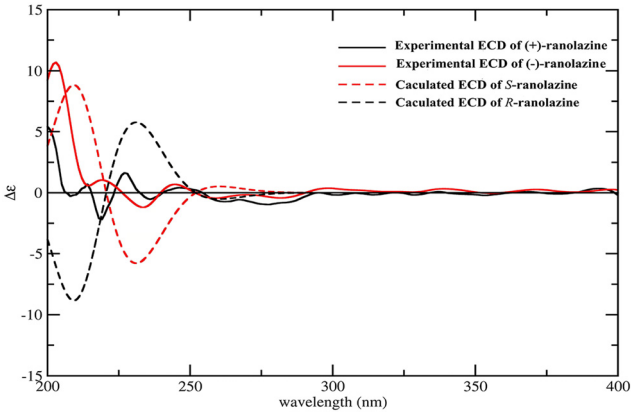

Fig. 3 Experimental and calculated ECD spectra of ranolazine enantiomers.

3.5 Method validation

3.5.1 Specificity and carry-over. The specificity assay was assessed by comparing six different sources of blank samples with the corresponding spiked samples at the LLOQ level and the actual plasma or tissue. As displayed in Fig. 4, *rac*-ranolazine and IS had excellent peak shape and were well resolved, and there were no interfering peaks from endogenous substances near the retention times of ranolazine and IS, demonstrating the method's effective specificity.

For the carry-over effect, no significant signal response at the retention time of analytes and IS was observed in blank samples injected immediately following the analysis of the highest concentration samples, demonstrating a negligible carry-over effect of the proposed method.

3.5.2 Linearity and LLOQ. The calibration curves were validated in the concentration range of 2–100 ng mL^{-1} and 2–500 ng mL^{-1} for each enantiomer in plasma and tissue samples, respectively, with a correlation coefficient of >0.990. Based on a signal-to-noise ratio of >10, this assay offered an LLOQ of 2 ng mL^{-1} for individual enantiomer in plasma and tissue samples, and revealed a satisfactory level of accuracy (Table S1, ESI†).

3.5.3 Precision and accuracy. The outcomes of precision and accuracy, based on LLOQ and three QC levels, are presented in Table S1 (ESI†). At each concentration level, the RSD values of intra- and inter-day precision were <14.0% and the accuracy results (RE) ranged from −10.0% to 10.0%. These results were within the acceptance criteria.

3.5.4 Extraction recovery and matrix effect. The mean extraction recoveries and matrix effect of *R*-(+)- and *S*-(−)-ranolazine

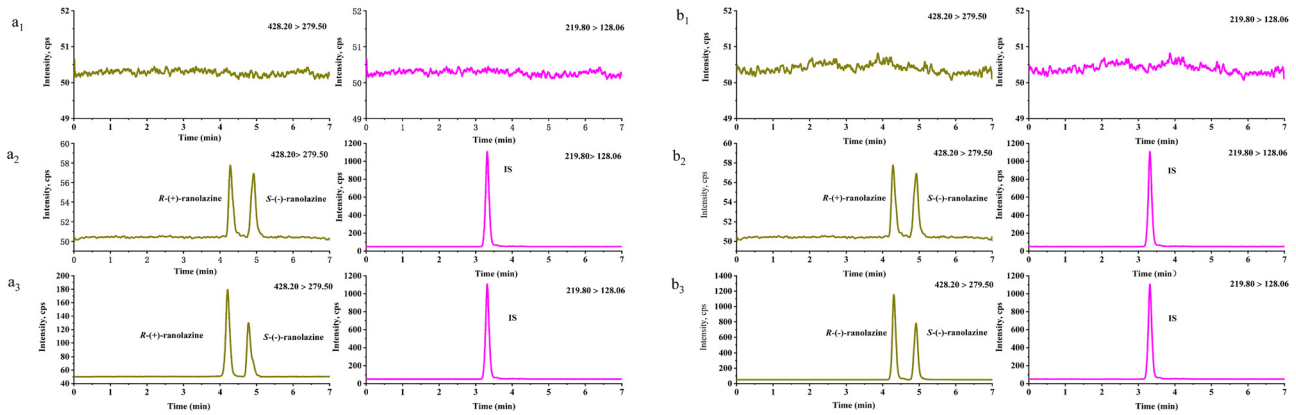

Fig. 4 Representative MRM chromatograms of ranolazine enantiomers and IS in rat plasma and tissue samples: (a_1) a blank plasma sample and (b_1) blank kidney homogenate, (a_2) a blank plasma sample spiked with *rac*-ranolazine at a LLOQ of 2 ng mL^{-1} per enantiomer and (b_2) blank kidney homogenate spiked with *rac*-ranolazine at the LLOQ of 2 ng mL^{-1} per enantiomer and IS, (a_3) an actual plasma sample at 0.5 h and (b_3) actual kidney extract at 12 h after oral administration of 15 mg kg^{-1} *rac*-ranolazine extended-release tablets.

in plasma and tissue samples are indicated in Table S2 (ESI†). The mean recoveries for *R*-(+)-ranolazine and *S*-(−)-ranolazine at three QC levels ranged from 95.3% to 104.3% and 95.5% to 103.7%, respectively. The LLE procedure using MTBE could achieve a satisfactory relatively consistent recovery of ranolazine enantiomers in plasma and tissue samples.

Considering the matrix effect, the NMF was within the range of 96.3–104.3% for ranolazine enantiomers and IS with all RSD values <11.0%. The validation results revealed that the matrix effect on the ion suppression or enhancement from the plasma and tissue matrix was not significant under the existing conditions.

3.5.5 Stability. Table S3 (ESI†) summarizes the stability results of *R*-(+)- and *S*-(−)-ranolazine in plasma and tissue samples under four storage conditions. The RE values of each enantiomer in plasma and tissue samples ranged from −12.3% to 12.4% for *R*-(+)-ranolazine and −12.1% to 13.0% for *S*-(−)-ranolazine, and RSD values were <12.0%, suggesting that the analytes were stable throughout the validation process.

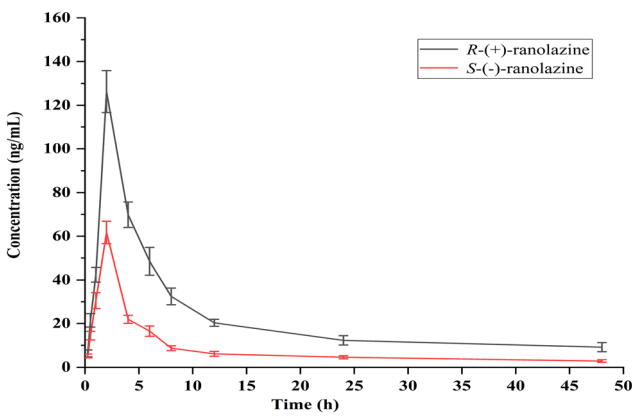

Fig. 5 Mean plasma concentration–time curves of *R*-(+)- and *S*-(−)-ranolazine following oral administration of 15 mg kg^{-1} *rac*-ranolazine extended-release tablets to SD rats. Each point represents the mean ± SD (n = 6).

Table 1 Pharmacokinetic parameters of *R*-(+)- and *S*-(−)-ranolazine after oral administration of 15 mg kg^{-1} *rac*-ranolazine extended-release tablets to SD rats (mean ± SD, n = 6)

	Mean ± SD		*T*-test
Parameters	*R*-(+)-ranolazine	*S*-(−)-ranolazine	
C_{max} (ng mL^{-1})	126.28 ± 9.65	61.68 ± 5.14	*
T_{max} (h)	2.00 ± 0.33	2.00 ± 0.33	—
$t_{1/2}$ (h)	10.35 ± 1.53	32.79 ± 6.39	*
AUC_{0-t} (ng h mL^{-1})	1059.13 ± 88.72	388.94 ± 28.65	*
$AUC_{0-\infty}$ (ng h mL^{-1})	1096.70 ± 95.72	521.61 ± 71.54	*
CLz/F (L h^{-1} kg^{-1})	13.752 ± 1.14	29.16 ± 3.91	*
Vz/F (L kg^{-1})	204.836 ± 30.96	1359.28 ± 103.97	*

Values significant differences between *R*-(+)- and *S*-(−)-ranolazine (*: $p < 0.05$). C_{max}, the maximum plasma concentration. T_{max}, the time to reach the maximum plasma concentration. $t_{1/2}$, the half-life of elimination. AUC_{0-t}, area under the drug concentration–time curve to the last measurable concentration. $AUC_{0-\infty}$, area under the plasma drug concentration-time curve to infinity. CLz/F, apparent clearance. Vz/F, apparent volume of distribution.

3.6 Application to a stereoselective pharmacokinetic study

Our HPLC-ESI-MS/MS method was further applied in the pharmacokinetics study of ranolazine enantiomers in SD rats following oral administration of 15 mg kg^{-1} *rac*-ranolazine extended-release tablets. The quantified mean plasma concentration–time profiles of *R*-(+)- and *S*-(−)-ranolazine up to 48 h are presented in Fig. 5, and the corresponding pharmacokinetic parameters are given in Table 1. The pharmacokinetic parameters were compared using paired sample *T*-tests. The differences between parameters of *R*-(+)- and *S*-(−)-ranolazine were considered statistically significant if the *p*-value was <0.05. All data were presented as mean ± SD.

As observed in Fig. 5, concentrations of both enantiomers gradually increased in plasma following oral administration, achieving the C_{max} in <5 h. By comparing the drug concentration–time curves more precisely, we observed that the mean C_{max} value of *R*-(+)-ranolazine was 2.05 times higher than that of *S*-(−)-ranolazine, illustrating that *R*-(+)-ranolazine had stronger absorption capability. Moreover, the AUC_{0-t} and $AUC_{0-\infty}$ of

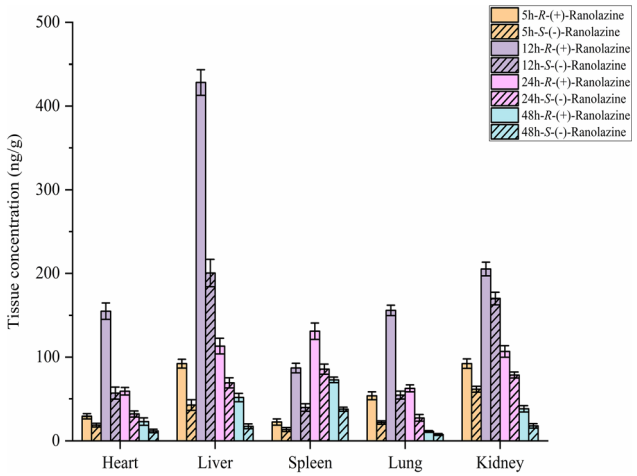

Fig. 6 Tissue distribution after oral administration of *rac*-ranolazine extended-release tablets at a single dose of 15 mg kg^{-1}. Data were presented as mean ± SD (n = 6).

R-(+)-ranolazine were 2.72 and 2.10-fold higher than those of *S*-(−)-ranolazine, respectively. These results completely corresponded to the stereoselective pharmacokinetic research of another azine drug, thioridazine, in which the *R*-isomer was entirely responsible for the higher concentration of the isomer.[35] Additionally, in the elimination phase, we observed a significant difference. The shorter half-life ($t_{1/2}$) of *R*-(+)-ranolazine allowed a relatively quick elimination in rat plasma. Conclusively, the stereoselectivity of ranolazine enantiomers in plasma pharmacokinetics of SD rats was observed in our study.

3.7 Application to enantioselective tissue distribution in SD rats

In this research, we first transformed the unit of ng mL^{-1} to ng g^{-1} to obtain the final tissue concentrations following oral administration of 15 mg kg^{-1} *rac*-ranolazine extended-release tablets. As presented in Fig. 6, except for the brain (lower than the level of LLOQ) either *R*-(+)- or *S*-(−)-ranolazine was widely distributed in all tissues with blood flow occurrence in the six representative tissues (including brain, heart, liver, spleen, lungs, and kidneys). This might be related to the poor ability of ranolazine to cross the blood–brain barrier of ranolazine.[36,37] By comparing the results more precisely, we observed that the liver was the main distribution organ, followed by the kidneys, heart, lungs, and spleen. The peak concentration time was observed at 12 h for the heart, liver, lungs, and kidneys (24 h for spleen), illustrating that the potential hepatotoxicity might have occurred in clinical treatment, providing scientific evidence for further research.[38,39] Moreover, significantly enantioselective differences in all target tissues were observed, and every time point indicated evidence of higher concentrations of *R*-(+)-ranolazine than its antipode, revealing that *R*-(+)-ranolazine possessed a slower metabolism rate and was more likely to be present in those target tissues than *S*-(−)-ranolazine. The determined concentrations of *R*-(+)-ranolazine in the heart, liver, spleen, lungs, and kidneys were 1.6–2.7, 1.6–3.0, 1.5–2.2, 1.5–2.9 and 1.2–2.1 times higher than those of *S*-(−)-ranolazine, respectively. This was consistent with the pharmacokinetic report. Concluding from the results of pharmacokinetics and tissue distribution, it was known that there were significant enantioselective differences between *R*-(+)- or *S*-(−)-ranolazine not only at the pharmacokinetic stage but also in tissue distribution.

4. Conclusion

An HPLC-ESI-MS/MS analysis method was established and validated for the determination of ranolazine enantiomers in biological samples, and the corresponding separation-related factors were explored and optimized in our study. After liquid–liquid extraction from the biological matrix, baseline resolution of the enantiomers was achieved on a Chiralcel OD-RH column within 6 min, which proved to be more efficient than the previously reported method. Our method was successfully applied to stereoselective pharmacokinetic analysis and tissue distribution following oral administration of 15 mg kg^{-1} *rac*-ranolazine extended-release tablets. Our pharmacokinetic outcomes demonstrated that *R*-(+)-ranolazine revealed stronger absorption capability than *S*-(−)-ranolazine. *R*-(+)-ranolazine also revealed a slower metabolism rate and was more likely to exist in those target tissues than *S*-(−)-ranolazine in the tissue distribution study. Our results indicated that ranolazine enantiomers displayed stereoselective disposition in both plasma and tissue distribution, which may aid in developing individual ranolazine enantiomers in the future.

Funding sources

This work was financially supported by the National Natural Science Foundation of China (82003971) and the China Postdoctoral Science Foundation (2021M692227).

Conflicts of interest

The author(s) declare(s) that they have no conflicts of interest to disclose.

Acknowledgements

The author wishes to thank Professor Xingjie Guo for rendering much assistance in the preparation of this manuscript.

References

1 B. B. Keseroglu, E. Ozer, T. Karakan, B. C. Ozgur, H. Surer, E. Ogus, S. Hucemenoglu, C. N. Yuceturk and K. Agras, *Andrologia*, 2020, **25**, e13616.
2 B. R. Chaitman, S. L. Skettino, J. O. Parker, P. Hanley, J. Meluzin, J. Kuch, C. J. Pepine, W. Wang, J. J. Nelson, D. A. Hebert and A. A. Wolff, *J. Am. Coll. Cardiol.*, 2004, **43**, 1375–1382.

3 C. J. Pepine, A. A. Wolff and R. S. Group, *Am. J. Cardiol.*, 1999, **84**, 46–50.
4 N. A. Undrovinas, V. A. Maltsev, L. Belardinelli, H. N. Sabbah and A. Undrovinas, *J. Physiol. Sci.*, 2010, **60**, 245–257.
5 H. Fukaya, B. N. Plummer, J. S. Piktel, X. P. Wan, D. S. Rosenbaum, K. R. Laurita and L. D. Wilson, *Heart Rhythm*, 2019, **16**, 281–289.
6 L. Belardinelli, J. C. Shryock and H. Fraser, *Heart*, 2006, **92**, iv6–iv14.
7 M. Cattaneo, A. P. Porretta and A. Gallino, *Int. J. Cardiol.*, 2015, **181**, 376–381.
8 E. Tagliamonte, F. Rigo, T. Cirillo, C. Astarita, G. Quaranta, U. Marinelli, A. Caruso, C. Romato and N. Capuano, *J. Echocardiogr.*, 2015, **32**, 516–521.
9 X. P. Luo, Z. D. Zhai, X. M. Wu, Y. P. Shi, L. R. Chen and Y. M. Li, *J. Sep. Sci.*, 2006, **29**, 164–171.
10 D. Guo, R. J. He, W. X. Su, Z. Q. Liang, W. G. Zhang and J. Fan, *Chirality*, 2022, **34**, 126–133.
11 L. J. Jing, K. J. Li, F. Qin, X. T. Wang, L. Pan, Y. J. Wang, M. S. Cheng and F. M. Li, *J. Sep. Sci.*, 2012, **35**, 2678–2684.
12 P. da Fonseca and P. S. Bonato, *Anal. Bioanal. Chem.*, 2010, **396**, 817–824.
13 A. Dhalla, K. Leung, J. Shryock and D. Zeng, PCT/US2008/060090, 2008.
14 Y. Ning, W. Zhen, Z. Fu, J. Jiang, D. Liu, L. Belardinelli and A. K. Dhalla, *J. Pharmacol. Exp. Ther.*, 2011, **337**, 50–58.
15 Y. Li, H. Q. Wang, R. L. Wang, X. Y. Lu, Y. Wang, M. X. Duan, H. Y. Li, X. H. Fan and S. F. Wang, *J. Chromatogr. B: Anal. Technol. Biomed. Life Sci.*, 2019, **1128**, 121777.
16 L. C. He and S. C. Wang, *Arch. Pharm. Res.*, 2003, **26**, 763–767.
17 P. R. Babu, K. N. Babu, P. L. H. Peter, K. Rajesh and P. J. Babu, *Drug Dev. Ind. Pharm.*, 2013, **39**, 873–879.
18 S. R. Abburu, M. L. P. R. Alapati, A. S. Dadhich and M. K. Rao, *J. Pharm. Biomed. Anal.*, 2016, **29**, 190–194.
19 Y. Liang, L. Xie, X. D. Liu, W. D. Chen, T. Lu, Y. Xiong and G. J. Wang, *Rapid Commun. Mass Spectrom.*, 2006, **20**, 523–528.
20 J. Zhong, X. Q. Liu, Y. Chen, X. P. Zhao, Y. S. Wang and G. J. Wang, *Chromatographia*, 2007, **63**, 123–127.
21 U. Bhaumik, A. Ghosh, A. K. Sarkar, A. Bose, P. S. Selvan and P. Sengupta, *J. Pharm. Biomed. Anal.*, 2008, **48**, 1404–1410.
22 J. P. Bidada, I. D. Gonjari, C. S. Raut and C. J. Bhutada, *Der Pharma Chem.*, 2011, **3**, 1–4.
23 J. Gao, L. X. Chen, Q. Wu, H. Li, S. Q. Dong, P. Qin, F. Yang and L. Zhao, *Chirality*, 2019, **31**, 669–681.
24 E. Delée, L. L. Garrec, I. Jullien, S. Béranger, J. C. Pascal and H. Pinhas, *Chromatographia*, 1987, **24**, 357–359.
25 R. A. Simões, T. Barth and P. S. Bonato, *Bioanalysis*, 2013, **5**, 171–183.
26 J. Zhou, B. Yang, J. Tang and W. Tang, *New J. Chem.*, 2018, **42**, 3526–3533.
27 E. Francotte, *J. Chromatogr. A*, 2001, **906**, 379–397.
28 R. Geryk, K. Kalíková, J. Vozka, D. Plecitá, M. G. Schmid and E. Tesařová, *J. Chromatogr. A*, 2014, **1363**, 155–161.
29 L. A. Papp, M. Foroughbakhshfasaei, B. Fiser, P. Horváth, E. Kiss, K. Sekkoum, Á. Gyéresi, G. Hancu, B. Noszál, Z. Szabó and G. Tóth, *Chirality*, 2020, **32**, 158–167.
30 Bioanalytical Method Validation Guidance for Industry From the United States Food and Drug Administration, 2018.
31 I. W. Wainer, R. M. Stiffin and T. Shibata, *J. Chromatogr. A*, 1987, **411**, 139–151.
32 Y. Okamoto and E. Yashima, *Angew. Chem., Int. Ed.*, 1998, **37**, 1020–1043.
33 M. Okamoto and H. Nakazawa, *J. Chromatogr. A*, 1991, **588**, 177–180.
34 M. Okamoto, *J. Pharm. Biomed. Anal.*, 2002, **27**, 401–407.
35 C. B. Eap, L. Koeb, K. Powell and P. Baumann, *J. Chromatogr. B: Biomed. Sci. Appl.*, 1995, **669**, 271–279.
36 T. I. F. H. Cremers, G. Flik, J. H. A. Folgering, H. Rollema and R. E. Stratford, *Drug Metab. Dispos.*, 2016, **44**, 624–633.
37 R. N. Prentice, M. Younus, W. Krittaphol-Bailey and S. B. Rizwan, *J. Sep. Sci.*, 2021, **44**, 2693–2704.
38 M. P. Grillo, J. C. M. Wait, M. T. Lohr, S. Khera and L. Z. Benet, *Drug Metab. Dispos.*, 2010, **38**, 133–142.
39 B. B. Gao, S. S. Zhao, H. Y. Shi, Z. X. Zhang, L. S. Li, Z. Z. He, Y. Wen, A. Covaci and M. H. Wang, *Environ. Int.*, 2020, **143**, 105940.